

Multivariate Flood Risk Assessment of the Unplanned Semi- Urban Region by Incorporating Flood Hazard, Vulnerability, and Exposure

Sachin Bhare (✉ studentsachinbhere@gmail.com)

Indian Institute of Technology Bombay <https://orcid.org/0000-0003-0670-4941>

M. Janga Reddy

Indian Institute of Technology Bombay

Research Article

Keywords: Flood risk, Vulnerability, Exposure, Hazard, Kulgoan-Badlapur Municipal Council, Ulhas River, vaccination, vaccines

Posted Date: January 28th, 2022

DOI: <https://doi.org/10.21203/rs.3.rs-1286315/v1>

License:  This work is licensed under a Creative Commons Attribution 4.0 International License.

[Read Full License](#)

1
2
3
4
5
6
7
8
9
10
11
12
13
14
15
16
17
18
19
20
21
22
23
24
25
26
27
28
29
30
31
32
33
34
35
36
37
38

Multivariate flood risk assessment of the unplanned semi- urban region by incorporating flood hazard, vulnerability, and exposure

Sachin Bhare^{1*} and M. Janga Reddy^{1,2}

¹Department of Civil Engineering, Indian Institute of Technology Bombay, Mumbai.

²Interdisciplinary Program (IDP) in Climate Studies, Indian Institute of Technology Bombay, Mumbai.

Corresponding Author

Sachin Bhare*

Address: Department of Civil Engineering, Indian Institute of Technology Bombay, Powai, Mumbai, Maharashtra 400076, India.

Mobile No: +91 9768928318

Email: 204040025@iitb.ac.in

39 **ABSTRACT**

40 The mapping of flood risk is important to identify areas at risk and to improve flood disaster management and
41 preparedness. Flood risk is often expressed as the product of the hazard and the probable consequences which is
42 determined in terms of direct damages by assessing flood vulnerability and exposure. This study aims to develop
43 the flood risk assessment (FRA) framework for the dense semi-urban region by incorporating flood hazard,
44 topographic and socio-economic vulnerability, along with exposure, which is calculated by considering housing
45 conditions and classification of the damages by different land use and land cover classes. The FRA at the
46 municipal level is challenging due to the spatial resolution of social, economic, and medical indicators therefore
47 this study attempts to map the flood risk of the semi-urban region where the different zones and housing
48 communities are intertwined due to a lack of town planning. This FRA framework is applied to the Kulgoan-
49 Badlapur Municipal Council (KBMC) located at the Ulhas Riverbank, a west-flowing river in Maharashtra,
50 India. The city is located at the riverbank, which receives more than 2000 mm rainfall annually, and as most
51 growing industries and businesses depend on the river itself, the risk associated with flood increases
52 exponentially. The study shows that the spatial distribution of the flood risk is higher in the wards which are
53 densely populated and near the river stream. Despite low population and assets, some neighborhoods are highly
54 susceptible to flood due to their topographical conditions. Over the years, the population has been increasing in
55 the neighborhoods due to the new real estate projects, which will make them more vulnerable to floods, and the
56 overall risk is increasing. Study shows that the 82% of the area of Valavli and Manjarli ward comes under high
57 flood risk due to high topographic vulnerability and exposure. Similarly the few parts of Industrial zone also
58 comes under the high risk because of its location near river bank. The wards like Kulgaon comes under medium
59 flood risk despite its high socio-economic vulnerability and high exposure which proves that the flood risk is
60 majorly depends on the flood inundation. The exposure-based flood risk assessment will help to frame a more
61 practical and reasonable evaluation of risk for growing urban and industrial zones.

62 **Keywords:** Flood risk; Vulnerability; Exposure; Hazard; Kulgoan-Badlapur Municipal Council; Ulhas River.

63

64 **1. INTRODUCTION**

65 A flood is defined as the water overflow from river banks to the adjoining area. The damage caused by floods in
66 terms of loss of life, property, and economic loss is all too well known (Merz et al. 2010; Nofal and van de Lindt
67 2020; Sen, Dutta, and Laskar 2021; Svetlana, Radovan, and Ján 2015). Floods have a huge impact than any
68 other disaster event and have a high destructive potential to alter the ecology, and it can cause social and
69 economic damages. Floods are one of the disastrous extreme hydrological events responsible for the thousands
70 of casualties worldwide and billion dollars of economic damage (Komolafe, Herath, and Avtar 2018; Mokhtari,
71 Soltani, and Mousavi 2017)With an increase in population every year, more and more flood-prone areas are
72 occupied for residential, agricultural, and industrial activities. Under normal conditions, the area was used for
73 floodwater storage now has become build-up areas, leading to frequent flooding of these areas and the
74 possibility of large-scale economic damages (Grigg 2020; Koks et al. 2015).

75 In the past, different studies expressed the flood risk as a function of flood hazard and vulnerability which
76 analyzes the intensity of the flood and the damage caused to the assets (Ali, Bajracharya, and Koirala 2016;
77 Jato-Espino et al. 2018). In the last two decades, the FRA is improved from a one-dimensional hazard
78 assessment to a multi-dimensional risk assessment considering the factors such as social and economic

79 vulnerability(Bengal, Chakraborty, and Mukhopadhyay 2019; Ghosh and Kar 2018; Nguyen et al. 2021; Sahoo
80 and Sreeja 2017; Tripathy et al. 2020a). The advances in the capacity of computational resources help to
81 incorporate multiple parameters responsible for the flood risk (Doorga et al. 2022; Monteil et al. 2022). In
82 single-dimensional FRA, the flood hazard is considered as one of the following factors like rainfall intensity,
83 flood inundation, flood depth, and rising sea level in coastal flooding. The multivariable FRA depends on the
84 flood hazard, vulnerability, and exposure, structural and non-structural measures as flood preparedness. Along
85 with the hazard, flood vulnerability is essential in assessing the possible damage due to flood events (Bengal,
86 Chakraborty, and Mukhopadhyay 2019; Franci et al. 2016; Kabenge et al. 2017). The socio-economic
87 conditions can be considered to evaluate the vulnerability and compute the direct and indirect damages. The
88 flood exposure still hasn't been incorporated well in the flood risk framework, maybe because it requires
89 combining the quantitative and qualitative data(Imran et al. 2019; Kittipongvises et al. 2020; Mohanty, Mudgil,
90 and Karmakar 2020).

91 The FRA for the unplanned semi-urban region is challenging due to homogenous socio-economic conditions,
92 which makes it difficult to divide the municipal council into different zones. The study attempts to classify the
93 wards of the municipal council based on various indicators which are responsible for flood vulnerability and
94 exposure. In this study, the flood risk of the Kulgoan Badlapur municipal council (KBMC), Maharashtra, India
95 is assessed by incorporating flood exposure with socio-economic and topographic vulnerability and flood
96 hazard. The KBMC is located near Western ghat, India, and The Ulhas River flows through the KBMC, which
97 is the home of around 18.4 million people, according to the 2011 census. Due to its location in the Mumbai
98 metropolitan region (MMR) and the industrial zone, the population is increasing. As the city is located at the
99 river bank and most growing industries and businesses depend on the river itself, the flood vulnerability
100 increases exponentially. For FRA, several studies majorly focused on the flood hazard and vulnerability, which
101 fails to assess the possible direct and indirect damages to the infrastructure and industrial zone. Therefore, the
102 main objective of this study is to incorporate the exposure associated with the industrial zone and infrastructure
103 into the risk assessment framework along with socio-economic vulnerability. Along with the main objective
104 following are the some objectives of the study:

- 105 • This study aims to develop the FRA framework for the unplanned semi-urban region by incorporating
106 flood hazard, socio-economic, topographic, and medical vulnerability along with infrastructural
107 exposure.
- 108 • To develop the flood risk map at ward level for municipal councils to allocate the resources for the
109 flood mitigation.
- 110 • To assess the risk involved with the different resources in terms of direct probable damages by
111 including the flood exposure based on the different land use and zones in municipal council.

112 The flood hazard is considered as the flood inundation simulated using the HEC-RAS model. The vulnerability
113 is calculated by considering different topographic and socio-economic parameters using Analytical Hierarchy
114 Process (AHP), and the exposure is calculated by considering plinth height, road network density, and type of
115 buildings. The following sections discuss the proposed framework for flood risk assessment, and the subsequent
116 section presents the application of the proposed FRA framework for the KBMC region, and the corresponding
117 results are discussed focusing on evaluating different flood risk parameters for each ward of the KBMC area.

118

119

120 2. METHODOLOGY

121 The risk is expressed as the expected loss of life, property damage, disruption of economic activity,
122 environmental damage, etc (Barrett, Steinbach, and Addison 2021). This provides the base for the multi-
123 dimensional flood risk assessment in which the consequences in terms of expected losses are essential to
124 calculate and interpret flood risk effectively along with the flood hazard. This study incorporates topographic,
125 socio-economic vulnerability, and exposure for semi-urban unplanned municipal council and **Figure 1** shows
126 the flow chart of the proposed framework.

127 The flood hazard is calculated by classifying the risk level of flood inundation, and the assessment of
128 consequences are divided into vulnerability and exposure. The vulnerability is determined based on the
129 combined index of topographic factors, socio-economic factors, and medical indicators similarly the exposure is
130 calculated using two indicators, viz., indicator based on road networks across cities and housing types, and the
131 other indicator based on the degree of importance of the land use and land cover classes. Finally the FRA can
132 be interpreted mathematically as the product of flood hazard, vulnerability, and exposure.

133 The flood hazard is calculated considering the flood inundation extent corresponding to different return periods
134 (50-year, 100-year, and 200-year). The flood magnitude of the various return period is calculated using
135 Intensity-Duration-Frequency (IDF) curve. The flood hazard assessment in various studies involved the
136 determination of the flood inundation, estimating the peak discharge and associated water levels, along with the
137 probability of the extreme rainfall or discharge (Cançado et al. 2008; Díez-Herrero and Garrote 2020; Ganguli
138 and Reddy 2013; Koks et al. 2014; Kron 2002; Molinari et al. 2019; Tripathy et al. 2020b; Wang et al. 2019).
139 To estimate the flood hazard, few studies proposed the multi-criteria methods, which calculate the hazard based
140 on the different factors associated with it. This type of calculation is more suitable for the spatial analysis of the
141 hazard, where the observed discharge and associated water levels data are not available. Figure 2 shows the flow
142 chart of methodology for mapping of the flood hazard.

143 For calculating the flood extent, steady flow hydraulic modeling is performed using the HEC-RAS model. The
144 HEC-RAS model uses energy, continuity, and momentum equations with an iterative procedure using the
145 standard step method (USACE 2016). The HEC-RAS model computes the flood water elevation by taking
146 inputs of the geometrical data and discharge values for different rainfall intensities, and the discharge values at
147 all reaches, junctions, and watersheds are computed using the hydrological model, HEC-HMS (Feldman 2000).
148 The HEC-HMS uses the SCS-CN method for calculating the runoff volume in which the rainfall data and the
149 CN grid are required as the model's input. The 50 years, 100 years, and 200 years rainfall intensities are
150 calculated using Intensity-Duration-Frequency (IDF) curves (Kothyari and Garde 1992) in which the hourly
151 rainfall data of Indian Meteorological Department's (IMD) is used. After calculating the rainfall intensities, the
152 values are used as an input in the calibrated HEC-HMS model. The discharge values are incorporated into the
153 HEC-RAS model to estimate the flood inundation extent for 50 years, 100 years, and 200 years which then
154 divided into different hazard zones. After calculating the flood hazard the flood vulnerability is calculated based
155 on two aspects: The city's physical and topographical conditions and the socio-economic condition to bear the
156 shocks after flood events or to understand the resilience towards floods. **Figure 3** shows the flow chart for
157 determining the high and low vulnerable zones in the municipal council.

158 To calculate the topographic vulnerability, factors like elevation, slope, distance from the river, drainage
 159 density, flow accumulation, topographic wetness index (TWI), Stream power index (SPI), and curvature are
 160 considered. The elevation is the factor that influences highly as compared to the other parameters. The low
 161 elevation area has a high probability of getting flooded as compared to the high elevation. The distance from
 162 river and drainage density are key parameters to understand the extent and time for the flood water to reach into
 163 the city. The topographic wetness index (TWI) is calculated to understand the probable flood inundation regions
 164 in the basin which is calculated using Moore's equation (Moore, Grayson, and Ladson 1991). Other factors like
 165 flow accumulation, curvature, and stream power index (SPI) also help to determine the critical regions
 166 vulnerable to floods. To calculate the combined topographic vulnerability index, the Analytical Hierarchy
 167 Process (AHP) is used.

168 The AHP method introduced by (Saaty 1987) which uses the pairwise comparison matrix to calculate the
 169 weightage of each parameter to establish the vulnerability map. The comparison between different parameters is
 170 made by assigning the numerical values to each component based on the relevance and significance (Bengal,
 171 Chakraborty, and Mukhopadhyay 2019; Chen, Yeh, and Yu 2011; Danumah et al. 2016; Ghosh and Kar 2018;
 172 Hu et al. 2017; Lin, Wu, and Liang 2019; Ramkar and Yadav 2021). **Table 1** shows the pairwise comparison of
 173 different topographic parameters. For example, '1' is for the equally significant, 3 for moderately more
 174 significant, 5 for strongly more significant, and 7 for very strongly more significant. And 2, 4, and 6 are the
 175 intermediate scores. **Table 2** shows the normalized weightage of each topographic parameter.

176 The steps involved in the AHP procedure for calculating the weightages is given below:

- 177 1. Identify the important factors and/or parameters in the flooding problem.
- 178 2. Arranging the parameters into hierarchical order based on each parameter's influence on the flood
 179 vulnerability.
- 180 3. According to the relevance of the factors, the numerical value is assigned from 1 to 7.
- 181 4. A comparison matrix is built, and the eigenvector computes the normalized weights.

182 The comparison matrix is built with the diagonal elements being equal to 1, using the following expression:

$$183 \quad A = (a_{ij})_{m \times n} = \begin{bmatrix} a_{11} & a_{12} & \dots & a_{1n} \\ a_{21} & a_{22} & \dots & a_{2n} \\ \vdots & \vdots & \ddots & \vdots \\ a_{n1} & a_{n2} & \dots & a_{nn} \end{bmatrix},$$

$$184 \quad a_{ii} = 1, a_{ij} = \frac{1}{a_{ji}}, a_{ij} \neq 0 \quad (1)$$

185 The consistency of the AHP method is assessed using consistency ratio (CR). Following is the expression for
 186 CR (Saaty 1987):

$$187 \quad CR = \frac{\text{Consistency Index (CI)}}{\text{Random Index (RI)}}, \quad CR < 0.10 \text{ is acceptable} \quad (2)$$

$$188 \quad \text{Where, } CI = \frac{\lambda_{\max} - n}{n - 1}, \lambda_{\max} = \text{Principal eigenvalue of the matrix} \quad (3)$$

189 The Random Index (RI) is determined by the number of parameters in the comparison matrix. The value of RI is
 190 referred from the table given in Saaty's 1980 work on the AHP. Each topographic factor is divided into five
 191 categories, and the sub-criteria AHP analysis is done for every element to neglect the effect of the different
 192 units. **Table 3** presents the sub-criteria pairwise comparison matrix of each parameter.

193 Along with the topographic vulnerability, the socio-economical plays an essential role in understanding indirect
 194 flood damages. The factors such as total population, population density, household income, and medical

195 indicator which is based on the percentage of the people vaccinated against the flu, etc., are considered as key
 196 factors to understand the spatial distribution of the vulnerability. The choice of indicator for the vulnerability
 197 depends on the demographic data availability. Some indicators are positive in terms of flood vulnerability,
 198 which increases the vulnerability with an increase in the values, for example, the total population across
 199 different wards, population density, and the number of houses. Some indicators help to reduce the flood
 200 vulnerability as the percentage of vaccination of the dependant population, interprets the region's health
 201 condition. High vaccination percentage indicates the low vulnerability of the people to water-borne diseases due
 202 to floods. The combined vulnerability index is then calculated by assigning a weight to each factors based on
 203 how they influence the flood vulnerability, more or less. Using the standardization approach, the parameters are
 204 converted into a scale from maximum to minimum by assigning 1 to 0. Considering V_i as each indicator's pixel
 205 value, V_{max} , and V_{min} are the maximum and minimum values of the parameter, the standardized parameters
 206 (V_{std}) for negative and positive indicators are estimated by following formulas (Tripathy et al. 2020b).

$$207 \quad V_{std} = \frac{V_i - V_{min}}{V_{max} - V_{min}} \quad (Negative \ Indicator) \quad (4)$$

$$208 \quad V_{std} = \frac{V_{max} - V_i}{V_{max} - V_{min}} \quad (Positive \ Indicator) \quad (5)$$

209 The combined vulnerability index (Vul) is calculated by assigning the weightages w_1 and w_2 to the topographic
 210 vulnerability index (Vul_{topo}) and socio-economical vulnerability index (Vul_{SE}), respectively.

$$211 \quad Vul = W_1 * Vul_{topo} + W_2 * Vul_{SE} \quad (6)$$

212 Along with the vulnerability, the exposure is also incorporated for calculating the flood risk. The exposure helps
 213 to narrow down the vulnerability that can predict the state of direct damages due to floods.

214 Exposure is as significant as calculating flood hazard and vulnerability for analysing the flood risk. The
 215 exposure is calculated by considering two major factors. The first factor deals with the type of land use that
 216 comes under the flood extent based on the degree of importance, and the second is based on the building and
 217 infrastructure condition. **Figure 4** shows the flowchart for calculating the exposure.

218 Many unplanned municipal corporations in India have different zones which are intertwined like industrial
 219 zones, built-up, plantation, forest, and at some places, agricultural land too. Each land uses have a different level
 220 of importance based on its operation, economic output, and the number of people associated with it. Considering
 221 all factors, the degree of importance is assigned to land use and land cover classes ranging from 0 to 1. For
 222 example, the Industrial zone is considered high exposure to flooding due to possible severe direct damages, and
 223 therefore the high degree of importance is assigned to it. **Table 4** shows the degree of importance (D_i) to each
 224 land use and zones.

225 The second component of the exposure is the exposure of buildings and infrastructure (E_{BI}). It is calculated by
 226 considering the building's usable plinth height (H_p), type of building (Residential Complex, Single residential
 227 building, industrial building units, small houses, other institutional buildings), and road density (R_d). The
 228 attribute table is created for each building and infrastructure, and based on the above factors, the combined
 229 exposure value is calculated. For plinth height (H_p), the buildings are identified with ground-floor apartments
 230 and ground-floor stilt parking. The buildings with ground-floor apartments are considered to have high exposure
 231 to the flood as compared to the stilt parking facilities. Most of the residential complexes have a usable floor
 232 above 5 meters from ground level, which is less exposed to the flood. The single residential buildings with
 233 ground-floor apartments have high exposure value. Small individual houses are also considered under high flood

234 exposure. Compared to each pixel's 100-year flood depth (D_{100}), the apartment's height or usable floor height is
 235 calculated as corrected plinth height (H_{PC}). The standardization is done, considered as 'Exposure index for
 236 plinth' (EI_P), which is assigned to each building (0 to 1, for low exposure to high exposure). The formulas are
 237 given below:

$$238 \quad H_{PC} = \frac{\text{Plinth height } (H_p) - D_{100}}{D_{100}} \quad (7)$$

$$239 \quad EI_P = \frac{\text{Max}[H_{PC}] - H_{PC}}{\text{Max}[H_{PC}] - \text{Min}[H_{PC}]} \quad (8)$$

240 After calculating the exposure associated with the plinth height, the exposure index for building (EI_B) based on
 241 the type of building and amenities are determined. The numerical value of 0.25 is assigned to the residential
 242 complex, 0.5 is assigned to single residential buildings and industrial buildings, and 0.75 is for single small
 243 houses based on the level of exposure. Similarly, the exposure index for the road (EI_R) is calculated based on the
 244 road network and density. The standardization is done for each pixel based on the road density's maximum and
 245 minimum value (R_d). The higher road density leads to high flood exposure and vice versa. The following
 246 formulas give the exposure index for the road (EI_R) and total exposure value for building and infrastructure:

$$247 \quad EI_R = \frac{\text{Max}[R_d] - R_d}{\text{Max}[R_d] - \text{Min}[R_d]} \quad (9)$$

$$248 \quad E_{BI} = \frac{1}{3}(EI_P + EI_B + EI_R) \quad (10)$$

249 Exposure is the mean of values of the degree of importance for land use, and exposure associated with building
 250 and infrastructure (E_{BI}).

$$251 \quad \text{Exposure} = \frac{D_i + E_{BI}}{2} \quad (11)$$

252 Using the above equation, the spatial distribution of the exposure is calculated across the municipal council.
 253 After calculating the flood exposure, the flood risk is calculated using the following formula;

$$254 \quad \text{Flood risk} = \text{flood hazard} \times \text{flood vulnerability} \times \text{flood exposure} \quad (12)$$

255 The calculated flood risk represents the flood inundation and the direct damages caused by the inundation for
 256 different return periods, and the socio-economic ability of people and communities to mitigate the flood
 257 damages. The analysis also includes the infrastructural exposure, including the detailed analysis of plinth height,
 258 type of building, and the road network. The flood risk also consists of the damages to the industrial zone by
 259 giving a higher degree of importance. The proposed framework for flood risk assessment is applied to a case
 260 study of KBMC and a discussion of the results along with data collected and sources are presented in the
 261 following sections.

262

263 3. CASE STUDY AND DATA COLLECTION

264 The proposed framework is applied to the Kurla-Badlapur Municipal Council (KBMC) located at the bank of
 265 the Ulhas River, which is a west-flowing river in India. This section discusses the study area and data collected
 266 to determine the flood risk across the municipal council. The Ulhas basin is home to millions people in 6 major
 267 municipal corporations like Thane, Kalyan-Dombivili, Ulhasnagar, Bhiwandi-Nijampur, Badlapur, and
 268 Ambernath, which makes it the most populated district in the country, and any small natural calamity can lead to
 269 massive social and economic disaster (Das 2019a; Das and Pardeshi 2018; Kim et al. 2019; Rangari et al.
 270 2019) Flooding is very frequent in the basin due to its location in the high monsoon region. Due to unplanned
 271 urbanization and the climate change the 25-year floods are coming at 10-year frequencies, and the Urban

272 Planning officials are requesting the revised flood guidelines for new building sanctions. It is also observed that
273 the flood line of 17.5 Meters is crossed thirteen times from the year 1991 at the KBMC observation point.

274

275

276 **3.1 DATA COLLECTION**

277 The flood risk is calculated by determining the flood hazard, its associated topographic and socio-economic
278 vulnerability, and flood exposure. The flood hazard is estimated based on the inundation corresponding to
279 different return periods using hydrological and hydraulic modeling. To calculate the rainfall intensity for
280 different return periods, the Indian Meteorological Department's (IMD) rainfall data over the Ulhas river Basin
281 is used. The watershed is delineated using the ArcHydro tool for hydrological modeling by inputting 30-meter
282 resolution SRTM's digital elevation model (DEM) data, the land use, and soil map are required for generating a
283 CN grid to calculate the losses. The land use and land cover maps are generated using the Landsat data of 30 m
284 and 100 m resolution and the soil map is extracted from the FAO's Global soil map. The model is then
285 calibrated and validated using the observed discharge data of the Badlapur hydro-metro station. After
286 calculating the corresponding discharge for various rainfall intensities and return periods, the values are
287 incorporated into the HEC-RAS model. The geographical data is extracted and mapped in the HEC-GeoRAS
288 tool of ArcGIS, including rivers, channels, and cross-sections that form key input data sets to the HEC-RAS
289 model to run the steady flow analysis to determine the flood inundation (flood hazard). For calculating the
290 extent of flood inundation, the Digital Surface Model (DSM) of the Advanced Land Observing Satellite (ALOS)
291 DSM product of 30 meters (AW3D30) is used, which is available on the JAXA web portal as a base map. The
292 vulnerability is calculated considering topographic and socio-economic factors. Topographic vulnerability
293 factors like elevation, slope, topographic wetness index, stream power index, flow accumulation, and curvature
294 are derived from the SRTM's DEM of 30-meter resolution. The other factors, including distance from the river
295 and drainage density, are calculated from the river shapefiles. For socio-economic vulnerability, population
296 density, household income, and medical indicators based on the vaccination data for flu are considered. The
297 population data is downloaded from the World-pop data portal of 100-meter spatial resolution. The population
298 data is available as the people per pixel, which is calculated based on the random forest approach with
299 Remotely-Sensed and Ancillary Data (Stevens et al. 2015). For medical indicators, the vaccination data is used.
300 The data shows the percentage of the children taking vaccines for flu, based on the study conducted on
301 childhood vaccination performed in middle and low-income countries (Utazi et al. 2018). The household income
302 data is collected by the survey of municipal corporations, based on local taxes.

303 For exposure, urban divisions based on the land use data, road network, and condition of the buildings focusing
304 on the plinth height and construction type are considered. The road network and building's shapefile are
305 downloaded from the OpenStreetMap portal developed by the OpenStreetMap foundation and local survey
306 conducted by the KBMC. The application and the results are discussed in the following section for FRA of
307 KBMC.

308

309 **4. APPLICATION AND RESULTS**

310 The proposed methodology is applied to the Kulgaon Badlapur Municipal council (KBMC), considering hazards
311 as flood inundation, socio-economic and topographic vulnerability, and exposure by considering building plinth

312 height and different land use and land cover classes based on the degree of importance. At a resolution of 30
313 meters, the risk index is calculated for each pixel. The KBMC includes Urban, Semi-urban, Rural settlements
314 and different land use classes, like industrial zones, agricultural land, and Built-up land and each of the
315 categories has a different capacity to withstand the damages caused due to floods. This section discusses the
316 findings of the different flood risk factors, viz., flood hazard, vulnerability, and exposure of each ward which
317 helps to understand the spatial distribution of the flood risk in the KBMC.

318 **4.1 FLOOD HAZARD ESTIMATION**

319 The flood hazard is calculated by determining the flood inundation for the different return periods of rainfall.
320 The IDF curve is plotted using Gumbel's equation with the help of hourly rainfall data collected from the Indian
321 Meteorological Department (IMD). The KBMC considers the extreme rainfall events of 100-year frequency for
322 identifying flood lines, and due to climate change and land use pattern change, the intensities are changing for
323 different return periods; therefore, the 200-year rainfall is also considered to determine the flood inundation.
324 **Figure 6** shows the intensity and duration of rainfall for different return periods (frequencies).

325 The graph shows the rainfall intensity as 172.04 mm, 145.42 mm, and 122.5 mm for return periods of 200-year,
326 100-year, and 50-year, respectively. With the IDF curve, extreme rainfall is calculated and used to determine the
327 flow in the channels and inundation area.

328 After calculating the different intensities of the rainfall, the values are considered as input into the HEC-HMS
329 model to determine the discharge. The HEC-HMS model is calibrated with 30 years of the observed discharge
330 data from Badlapur hydro-meteorological station. The first ten years of observed discharge data are used for
331 calibration of the model, and the performance is evaluated by calculating the coefficient of determination (R-
332 squared) value. The model shows a good correlation after calibration with the R-square value of 0.734, which
333 shows a good correlation between the simulated and observed flow. After calibration of the model, the discharge
334 is simulated at different reaches and junctions which is then incorporated into the HEC-RAS model for
335 determining the flood inundation for different return periods.

336 The flood hazard is the area inundated due to floodwater from the Ulhas River. The hazard is divided into three
337 classes. **Figure 7** shows the spatial extent of the flood inundation associated with different return periods. The
338 spatial extent of the 200-year flood is higher than a 50-year flood, but the area that comes under the extent of the
339 50-year flood boundary will be affected more frequently. Therefore the risk associated with a flood inundated
340 area of 50-years is higher than the 200-years. The map shows the majority of the flood inundation is happening
341 in the Badlapur, Valhivali, and Manjarli ward (central and south-east ward) of the municipal council. The least
342 affected wards are Kulgaon and Belavali (north-west ward), which have a maximum settlement. Due to the
343 increasing demand for residential apartments, the developers are constructing residential complexes in the high
344 flood hazard wards like Badlapur and Manjarli which will increase the overall flood risk. The flood hazard map
345 also shows that some part of the Maharashtra Industrial Development Council (MIDC) area, an industrial zone
346 of the KBMC, is flooded for 100-year flood events. The vulnerability is high in the MIDC area as most
347 industries have manufacturing units and the efficiency of those industries depends on factors like water supply,
348 electricity, transportation, and many others, which can be affected due to the flooding.

349 **4.2 FLOOD VULNERABILITY ASSESSMENT**

350 The flood vulnerability is calculated by considering topographic factors and socio-economic factors. The
351 topographic vulnerability is calculated to determine the flood susceptibility. The primary data used for

352 calculating the topographic vulnerability is the DEM data. Multiple factors are considered for calculating the
353 topographic vulnerability and the weightage is assigned using the AHP based multi-criteria decision analysis
354 method. Factors including elevation, slope, distance from the river, drainage density, Stream power index,
355 topographic wetness index, and curvature are used to calculate the combined topographic vulnerability. The
356 single index is formed by assigning the hierarchical priority and weightage. **Figure 8(A)** shows the spatial
357 distribution of topographic vulnerability for the KBMC area. It also shows the topographic vulnerability is
358 highly correlated to the elevation and distance from the river stream as it has higher weightage in the AHP
359 framework. The Central ward, which is parallel to the stream, is more vulnerable than any wards and the
360 Badlapur ward also shows high topographic vulnerability compared to the old settlement, which is planned and
361 developed considering the flood risk. Some region of MIDC also come under the topographically vulnerable
362 region. As the scope of future settlement in the wards like Badlapur and MIDC with high topographic
363 vulnerability, the overall risk of these wards will be high as compared to the other parts of the KBMC.
364 The total vulnerability is calculated by combining the topographic and socio-economic vulnerability. For socio-
365 economic vulnerability, the total population, population density, household income, and medical indicators as
366 percentage of vaccination against flu are considered. All the indices are standardized to a scale of 1 to 0 (high
367 vulnerable to low vulnerable) to form the final socio-economic index. **Figure 8(B)** shows the spatial distribution
368 of the socio-economic index of the KBMC. The wards with a high urban population and built-up land have high
369 vulnerability despite having good economic conditions compared to the other wards of the municipal council.
370 Here the average household income per pixel is considered, and therefore it can be seen that despite high
371 cumulative wealth in semi-urban regions, the average per capita income is less. The socio-economic
372 vulnerability also depends on the population density, which is higher in the Kulgaon, Shirgaon, and Badlapur
373 wards. The population of the industrial zone is underestimated because the census data included only the living
374 or residential population. Therefore, the vulnerability can be seen as lower than the other wards, which is not the
375 actual picture as a lot of people work in three 8-hour shifts, which makes it more vulnerable. The socio-
376 economic vulnerability can be reduced by adopting effective town planning, and the population across the city
377 can be managed by constructing and promoting effective residential projects across the different wards of the
378 municipal council. The vulnerability can also be reduced by improving medical facilities across the city.
379 **Figure 8(C)** shows the combined ward level vulnerability index standardized to the scale at 0 to 1 by combining
380 the topographic and socio-economic vulnerability. The vulnerability represents the topographic and socio-
381 economic ability to cope with the flood and to develop resilience. The wards with high population density near
382 the stream are under high flood vulnerability, ultimately under high flood risk. The map shows the settlements in
383 Kulgaon and Valivali have high flood vulnerability, and the Badlapur and Shirgoan have medium to high flood
384 vulnerability.

385 **4.3 FLOOD EXPOSURE ASSESSMENT**

386 The flood exposure is calculated using two indicators, first the land use, and land cover classes, by assigning the
387 degree of importance and second the exposure associated with the building and infrastructure. The exposure
388 further disintegrates the vulnerability by including certain factors for example the population density or total
389 population in each ward represents the residential population only and therefore, the population in the industrial
390 zone is low in records compared to other wards, which underestimates the vulnerability. Consequently, the
391 exposure is incorporated in the risk framework by classifying further into different land use and land cover

392 classes, and the degree of importance is assigned to each zones. **Figure 9(A)** shows the map of land use and
393 land cover classes along with their degree of importance. The degree of importance is assigned based on the
394 probable damage caused by the flood to different land use and land cover classes.

395 **Figure 9(A)** shows that a higher value is assigned to the MIDC ward, an industrial zone along with Kulgaon and
396 Shirgaon ward, which consists of built-up land, and agricultural zones.

397 Another parameter for calculating the exposure is the exposure associated with the building and infrastructure
398 (E_{BI}); the detailed explanation is given in the methodology section. For plinth height (H_p), the buildings are
399 identified with ground-floor apartments and ground-floor stilt parking. The buildings with ground-floor
400 apartments are considered to have high exposure to the flood as compared to the stilt parking facilities. Most of
401 the residential complexes have a usable floor above 5 meters from ground level, less exposed to the flood. The
402 single residential buildings with ground-floor apartments have high exposure value. Small individual houses are
403 also considered under high flood exposure. Along with the plinth, the type of building is also considered for
404 calculating the possible damage in terms of exposure. The numerical value of 0.25 is assigned to the residential
405 complex, 0.5 is assigned to single residential buildings and industrial buildings, and 0.75 is assigned for single
406 small houses. Another factor is by considering the road density which is calculated to understand the location of
407 buildings, institutes, and other infrastructures. The high road density interprets the high flood exposure. The
408 road density is calculated using the line density function and then standardized to the scale of 0 to 1 (low
409 exposure to high exposure). **Figure 9(B)** shows the exposure map associated with the road density.

410 The infrastructural exposure is calculated by taking an average of three infrastructural exposure indicators,
411 which are road density, plinth level, and type of building. The infrastructural exposure indicates the possible
412 direct damages to the buildings, roads, and industrial zones. The infrastructural exposure is then combined with
413 exposure calculated for land use and land cover based on degree of importance. **Figure 9(C)** shows the spatial
414 distribution of the flood exposure of the KBMC.

415 From **Figure 9(C)**, it can also be noted that the exposure of the MIDC ward, an industrial zone, is higher than
416 other wards of the municipal council. The exposure in the map indicates the possible direct damage to the
417 infrastructure, buildings, and resources. It shows the high possibilities of damages in the urban wards of the
418 municipal council because of the low plinth height of the buildings, and single ground floor apartments.

419 **4.4 FLOOD RISK ASSESSMENT**

420 The flood risk is assessed as the multiplication of flood hazard, vulnerability, and exposure. All the parameters
421 are converted into a scale of 0 to 1, low risk to high risk. **Figure 10** shows the spatial distribution of the flood
422 risk. It shows that highly populated wards and near the stream are at higher risk. The map shows the generalized
423 relative risk of the KBMC. The high flood risk can be seen in the Valavli and Manjarli ward. About 82% of the
424 area of these wards comes under very high to high flood risk zone, which is also validated with the information
425 and aid provided by the municipal council to these wards. The Badlpaur, Yeranjad, and Kulgaon also come
426 under high to medium flood risk zone as 38% of the area of these wards come under high to medium flood risk.
427 The industrial zone MIDC ward also comes under the high to the medium flood risk zone. The direct damage in
428 the industrial zone is higher but still, due to other factors, the overall risk is reduced as the ward have low
429 population density and high plinth of building due to industrial building construction bylaws. The flood risk of
430 the industrial zone is underestimated as the data regarding the actual damage is not available. Due to changes in
431 climate and land-use patterns, the risk is going to increase as the intensity of flood hazards is going to increase.

432 The wards like Badlapur and Shirgaon have more barren land, which has the potential for residential and
433 industrial constructions in the future, which will lead to increase in flood risk despite incorporating all the
434 factors which indicate the direct infrastructural damage and socio-economic capability to mitigate the flood, the
435 risk is highly dependent on the flood hazard.

436

437

438

439 **5. DISCUSSION**

440 The study presented an effective framework for flood risk assessment of unplanned semi-urban settlements by
441 incorporating infrastructural and industrial damages into the conventional flood risk framework. The flood risk
442 is expressed as the function of flood hazard, topographic vulnerability, socio-economic vulnerability, and
443 exposure. The flood inundation for different return periods is considered as flood hazard. The rainfall intensity-
444 duration-frequency (IDF) curves are developed using hourly rainfall data, and the discharge is simulated for the
445 extreme rainfall using the HEC-HMS model. The discharge values are then used to determine the corresponding
446 inundation by HEC-RAS hydraulic modeling. As the discharge data is not available for the reach passing
447 through the municipal council, and the simulated discharge is used to determine the inundation of the flood. In
448 this study using 1D hydraulic modeling, only water spread area is calculated, but the assessment can be
449 improved by considering multivariable flood hazards. The flood depth at various locations and the flow velocity
450 can be used to enhance overall flood hazard mapping, and the damages can be assessed accordingly.

451 In this study the vulnerability is calculated by considering two parameters, topographic vulnerability and socio-
452 economic vulnerability. The topographic vulnerability represents the flood susceptibility which is calculated
453 using the Analytical hierarchy process (AHP). The topographic vulnerability is calculated by considering
454 elevation, slope, drainage density, and distance from the river, curvature, stream power index, and topographic
455 wetness index. The weightage is calculated by making a pairwise comparison of each factor and the priority is
456 assigned based on previous research conducted for flood susceptibility (Das 2019b). The topographic
457 vulnerability assessment can be improved by using a fine resolution elevation grid or more parameters
458 responsible for high flow. The socio-economic vulnerability is calculated along with the topographic
459 vulnerability, considering factors like population density, household income, and medical indicators. The
460 accuracy of socio-economic vulnerability indicates the ability of individuals or communities to mitigate the
461 flood. The socio-economic vulnerability depends on the ground data for the population, demographics, and
462 economic condition. The indicator can be improved by using more fine resolution data with different social
463 indicators. The spatial distribution of socio-economic conditions in urban regions is difficult to interpret as the
464 population is very diverse, and the integration of social and economic conditions makes it more complicated to
465 assess the vulnerability of individual households. For the medical indicator the percentage of vaccination against
466 water-borne diseases are considered but more ground surveys and data will help to improve the assessment of
467 socio-economic vulnerability.

468 The primary economical source of KBMC is the industries located in the MIDC area. The economic
469 vulnerability of the region depends on the exposure of industries to flood, which is more and more inclusive of
470 electronics. The exposure is calculated by considering the industrial zone and the infrastructural condition of the
471 municipal council, along with the infrastructural exposure which is calculated by considering the plinth height

472 of buildings and its association with depth of 100-year flood, the road density, and type of buildings. The
473 buildings are divided into high elevated residential buildings, small houses, and industrial buildings. The risk is
474 more to the small houses and the buildings with low plinth height. Large residential complexes assigned the
475 ground floor to the parking make it less exposed to the flood, and the industrial buildings have a relatively high
476 plinth as compared to the small individual houses. Still, most industries have manufacturing units that require
477 heavy instruments operated on the ground floor, which makes them more exposed to the flood.
478 This study contributed for developing a framework for the flood risk of the municipal council, which has semi-
479 urban settlements along with industrial zones and agricultural land. Incorporating the exposure based on the land
480 use and land cover classes makes the framework more effective in calculating the overall flood risk of municipal
481 councils. The study also considered incorporating the corresponding plinth height with 100-year flood depth.
482 The flood risk in urban regions is more complicated than basin-scale flood risk assessment due to diverse socio-
483 economic conditions, which underestimated the vulnerability. Therefore incorporation of exposure based on
484 industrial zones and infrastructural condition give a better evaluation of flood risk. Further, the flood risk
485 assessment framework can be improved by incorporating the flood preparedness factors like available disaster
486 mitigation resources in each ward, which can ultimately help to understand the allocation of the resources in
487 different parts of the municipal councils.

488

489 **6. CONCLUSION**

490 The study presented a multi-dimensional approach for flood risk assessment. To map flood risk of the unplanned
491 semi-urban region, the socio-economic and medical factors and infrastructural exposure that indicate the
492 probable direct and indirect damages are essential elements. The intensity of the flood risk majorly depends on
493 the possible damages due to flood extent, which can be calculated with factors like population spread across the
494 municipal council and their socio-economic and medical condition. The flood risk mapping helps to understand
495 the high-risk and low-risk zones within the municipal council. The main conclusions of the study are:

- 496 • The proposed flood risk assessment framework includes some of the crucial yet neglected indicators
497 like the medical condition of the population to fight against the flu due to flood water and water-borne
498 diseases, which can classify under the flood preparedness of the authorities.
- 499 • The ward-wise flood risk maps generated in this study are very useful for the authorities for the disaster
500 funding and resources distribution at ward levels. With such zoning, the authorities can modify the
501 resource distributions in the municipal council.
- 502 • Mapping of the flood risk according to the land use and land cover classes shows the monitory
503 damages are different for each class, and the consequences of the risk cannot be defined solely based
504 on the socio-economic vulnerability. For example, the population distribution data considers the
505 residential population, and therefore, the industrial region cannot be included under a high-risk zone.

506 In the densely populated regions, where the different types of housing are intertwined in a single residential
507 zone it is difficult to map the flood risk. Therefore, the flood exposure based on the different types of
508 housing and their possible damages is important to include in the risk assessment framework.

509

510 **STATEMENTS AND DECLARATIONS**

511 **FUNDING:** The authors declare that no funds, grants, or other support were received during the
512 preparation of this manuscript.

513 **COMPETING INTEREST:** The authors have no relevant financial or non-financial interests to disclose.

514 **AUTHOR CONTRIBUTION:** All authors contributed to the study conception and design. Material
515 preparation, data collection and analysis were performed by Sachin Bhare. The first draft of the manuscript
516 was written by Sachin Bhare and all authors commented on previous versions of the manuscript. All authors
517 read and approved the final manuscript.

518

519 REFERENCES

520 Ali, Karamat, Roshan M. Bajracharya, and Hriday Lal. Koirala. 2016. "A Review of Flood Risk Assessment."
521 *International Journal of Environment, Agriculture and Biotechnology* 1(4): 1065–77.

522 Barrett, Sam, Dave Steinbach, and Simon Addison. 2021. *Assessing Vulnerabilities to Disaster Displacement A*
523 *Good Practice Review*.

524 Bengal, West, Subhankar Chakraborty, and Sutapa Mukhopadhyay. 2019. "Assessing Flood Risk Using
525 Analytical Hierarchy Process (AHP) and Geographical Information System (GIS): Application."
526 *Natural Hazards* 99(1): 247–74. <https://doi.org/10.1007/s11069-019-03737-7>.

527 Cançado, Vanessa, Lucas Brasil, Nilo Nascimento, and André Guerra. 2008. "Flood Risk Assessment in an
528 Urban Area : Measuring Hazard and Vulnerability." (January).

529 Chen, Yi Ru, Chao Hsien Yeh, and Bofu Yu. 2011. "Integrated Application of the Analytic Hierarchy Process
530 and the Geographic Information System for Flood Risk Assessment and Flood Plain Management in
531 Taiwan." *Natural Hazards* 59(3): 1261–76.

532 Danumah, Jean Homian et al. 2016. "Flood Risk Assessment and Mapping in Abidjan District Using Multi-
533 Criteria Analysis (AHP) Model and Geoinformation Techniques, (Cote d'ivoire)." *Geoenvironmental*
534 *Disasters* 3(1). <http://dx.doi.org/10.1186/s40677-016-0044-y>.

535 Das, Sumit. 2019a. "Geospatial Mapping of Flood Susceptibility and Hydro-Geomorphologic Response to the
536 Floods in Ulhas Basin, India." *Remote Sensing Applications: Society and Environment* 14(January): 60–
537 74. <https://doi.org/10.1016/j.rsase.2019.02.006>.

538 ———. 2019b. "Geospatial Mapping of Flood Susceptibility and Hydro-Geomorphologic Response to the Floods in
539 Ulhas Basin, India." *Remote Sensing Applications: Society and Environment*.

540 Das, Sumit, and Sudhakar D. Pardeshi. 2018. "Morphometric Analysis of Vaitarna and Ulhas River Basins,
541 Maharashtra, India: Using Geospatial Techniques." *Applied Water Science* 8(6): 1–11.
542 <https://doi.org/10.1007/s13201-018-0801-z>.

543 Díez-Herrero, Andrés, and Julio Garrote. 2020. "Flood Risk Assessments: Applications and Uncertainties."
544 *Water (Switzerland)* 12(8): 1–11.

545 Doorga, Jay R.S. et al. 2022. "GIS-Based Multi-Criteria Modelling of Flood Risk Susceptibility in Port Louis,
546 Mauritius: Towards Resilient Flood Management." *International Journal of Disaster Risk Reduction*

547 67(November 2021): 102683. <https://doi.org/10.1016/j.ijdr.2021.102683>.

548 Feldman, Arlen D. 2000. "Hydrologic Modeling System Technical Reference Manual." *Hydrologic Modeling*
549 *System HEC-HMS Technical Reference Manual* (March): 148.

550 Franci, Francesca et al. 2016. "Satellite Remote Sensing and GIS-Based Multi-Criteria Analysis for Flood
551 Hazard Mapping." *Natural Hazards* 83(1): 31–51.

552 Ganguli, Poulomi, and M. Janga Reddy. 2013. "Probabilistic Assessment of Flood Risks Using Trivariate
553 Copulas." *Theoretical and Applied Climatology* 111(1–2): 341–60.

554 Ghosh, Abhishek, and Shyamal Kumar Kar. 2018. "Application of Analytical Hierarchy Process (AHP) for
555 Flood Risk Assessment: A Case Study in Malda District of West Bengal, India." *Natural Hazards* 94(1):
556 349–68. <https://doi.org/10.1007/s11069-018-3392-y>.

557 Grigg, Neil S. 2020. "Uncertainty and Legal Foreseeability in Flood Risk Management." *ASCE-ASME Journal*
558 *of Risk and Uncertainty in Engineering Systems, Part A: Civil Engineering* 6(3): 06020001.

559 Hu, Shanshan, Xiangjun Cheng, Demin Zhou, and Hong Zhang. 2017. "GIS-Based Flood Risk Assessment in
560 Suburban Areas: A Case Study of the Fangshan District, Beijing." *Natural Hazards* 87(3): 1525–43.

561 Imran, Muhammad, Kalsoom Sumra, Syed Amer, and Syed Faisal. 2019. "International Journal of Disaster Risk
562 Reduction Mapping Flood Vulnerability from Socioeconomic Classes and GI Data : Linking Socially
563 Resilient Policies to Geographically Sustainable Neighborhoods Using PLS-SEM." *International Journal*
564 *of Disaster Risk Reduction* 41(July): 101288. <https://doi.org/10.1016/j.ijdr.2019.101288>.

565 Jato-Espino, Daniel, Nora Sillanpää, Ignacio Andrés-Doménech, and Jorge Rodriguez-Hernandez. 2018. "Flood
566 Risk Assessment in Urban Catchments Using Multiple Regression Analysis." *Journal of Water Resources*
567 *Planning and Management* 144(2): 04017085.

568 Kabenge, Martin, Joshua Elaru, Hongtao Wang, and Fengting Li. 2017. "Characterizing Flood Hazard Risk in
569 Data-Scarce Areas, Using a Remote Sensing and GIS-Based Flood Hazard Index." *Natural Hazards*
570 89(3): 1369–87.

571 Kim, Sangpil, Hong Gyoo Sohn, Mi Kyeong Kim, and Hyongki Lee. 2019. "Analysis of the Relationship
572 among Flood Severity, Precipitation, and Deforestation in the Tonle Sap Lake Area, Cambodia Using
573 Multi-Sensor Approach." *KSCE Journal of Civil Engineering* 23(3): 1330–40.

574 Kittipongvises, Suthirat et al. 2020. "AHP-GIS Analysis for Flood Hazard Assessment of the Communities
575 Nearby the World Heritage Site on Ayutthaya Island, Thailand." *International Journal of Disaster Risk*
576 *Reduction* 48(April): 101612. <https://doi.org/10.1016/j.ijdr.2020.101612>.

577 Koks, E. E., M. Bočkarjova, H. de Moel, and J. C.J.H. Aerts. 2015. "Integrated Direct and Indirect Flood Risk
578 Modeling: Development and Sensitivity Analysis." *Risk Analysis* 35(5): 882–900.

579 Koks, E E, B Jongman, T G Husby, and W J W Botzen. 2014. "ScienceDirect Combining Hazard , Exposure
580 and Social Vulnerability to Provide Lessons for Flood Risk Management." *Environmental Science and*

581 *Policy* 47: 42–52. <http://dx.doi.org/10.1016/j.envsci.2014.10.013>.

582 Komolafe, Akinola Adesuji, Srikantha Herath, and Ram Avtar. 2018. “Methodology to Assess Potential Flood
583 Damages in Urban Areas under the Influence of Climate Change.” *Natural Hazards Review* 19(2):
584 05018001.

585 Kothyari, Umesh C., and Ramchandra J. Garde. 1992. “Rainfall Intensity-Duration-Frequency Formula for
586 India.” *Journal of Hydraulic Engineering* 118(2): 323–36.

587 Kron, Wolfgang. 2002. “Keynote Lecture : Flood Risk = Hazard × Exposure × Vulnerability.” : 82–97.

588 Lin, Lin, Zening Wu, and Qihua Liang. 2019. “Urban Flood Susceptibility Analysis Using a GIS-Based Multi-
589 Criteria Analysis Framework.” *Natural Hazards* 97(2): 455–75. [https://doi.org/10.1007/s11069-019-](https://doi.org/10.1007/s11069-019-03615-2)
590 03615-2.

591 Merz, B, H Kreibich, R Schwarze, and A Thielen. 2010. “Review Article ‘ Assessment of Economic Flood
592 Damage .’” : 1697–1724.

593 Mohanty, Mohit Prakash, Sahil Mudgil, and Subhankar Karmakar. 2020. “Flood Management in India: A
594 Focussed Review on the Current Status and Future Challenges.” *International Journal of Disaster Risk
595 Reduction* 49(March): 101660. <https://doi.org/10.1016/j.ijdr.2020.101660>.

596 Mokhtari, Fahimeh, Saeid Soltani, and Seyed Alireza Mousavi. 2017. “ Assessment of Flood Damage on
597 Humans, Infrastructure, and Agriculture in the Ghamsar Watershed Using HEC-FIA Software .” *Natural
598 Hazards Review* 18(3): 04017006.

599 Molinari, Daniela et al. 2019. “Validation of Flood Risk Models: Current Practice and Possible Improvements.”
600 *International Journal of Disaster Risk Reduction* 33(May 2018): 441–48.
601 <https://doi.org/10.1016/j.ijdr.2018.10.022>.

602 Monteil, Charlotte et al. 2022. “Rethinking the Share of Responsibilities in Disaster Preparedness to Encourage
603 Individual Preparedness for Flash Floods in Urban Areas.” *International Journal of Disaster Risk
604 Reduction* 67(July 2021).

605 Moore, I. D., R. B. Grayson, and A. R. Ladson. 1991. “Digital Terrain Modelling: A Review of Hydrological,
606 Geomorphological, and Biological Applications.” *Hydrological Processes* 5(1): 3–30.

607 Nguyen, Huu Duy et al. 2021. “Predicting Future Urban Flood Risk Using Land Change and Hydraulic
608 Modeling in a River Watershed in the Central Province of Vietnam.” *Remote Sensing* 13(2): 1–24.

609 Nofal, Omar M., and John W. van de Lindt. 2020. “Probabilistic Flood Loss Assessment at the Community
610 Scale: Case Study of 2016 Flooding in Lumberton, North Carolina.” *ASCE-ASME Journal of Risk and
611 Uncertainty in Engineering Systems, Part A: Civil Engineering* 6(2): 05020001.

612 Ramkar, Preeti, and Sanjaykumar M. Yadav. 2021. “Flood Risk Index in Data-Scarce River Basins Using the
613 AHP and GIS Approach.” *Natural Hazards* 109(1): 1119–40. [https://doi.org/10.1007/s11069-021-04871-](https://doi.org/10.1007/s11069-021-04871-x)
614 x.

615 Rangari, Vinay Ashok, V. Sridhar, N. V. Umamahesh, and Ajey Kumar Patel. 2019. "Floodplain Mapping and
616 Management of Urban Catchment Using HEC-RAS: A Case Study of Hyderabad City." *Journal of The*
617 *Institution of Engineers (India): Series A* 100(1).

618 Saaty, R. W. 1987. "The Analytic Hierarchy Process-What It Is and How It Is Used." *Mathematical Modelling*
619 9(3-5): 161-76.

620 Sahoo, Sanat Nalini, and Pekkat Sreeja. 2017. "Development of Flood Inundation Maps and Quantification of
621 Flood Risk in an Urban Catchment of Brahmaputra River." *ASCE-ASME Journal of Risk and Uncertainty*
622 *in Engineering Systems, Part A: Civil Engineering* 3(1): 1-11.

623 Sen, Mrinal Kanti, Subhrajit Dutta, and Jahir Iqbal Laskar. 2021. "A Hierarchical Bayesian Network Model for
624 Flood Resilience Quantification of Housing Infrastructure Systems." *ASCE-ASME Journal of Risk and*
625 *Uncertainty in Engineering Systems, Part A: Civil Engineering* 7(1): 04020060.

626 Stevens, Forrest R., Andrea E. Gaughan, Catherine Linard, and Andrew J. Tatem. 2015. "Disaggregating Census
627 Data for Population Mapping Using Random Forests with Remotely-Sensed and Ancillary Data." *PLoS*
628 *ONE* 10(2): 1-22.

629 Svetlana, Dobrovičová, Dobrovič Radovan, and Dobrovič Ján. 2015. "The Economic Impact of Floods and
630 Their Importance in Different Regions of the World with Emphasis on Europe." *Procedia Economics and*
631 *Finance* 34(15): 649-55.

632 Tripathy, Shrabani S., Hari Vittal, Subhankar Karmakar, and Subimal Ghosh. 2020a. "Flood Risk Forecasting at
633 Weather to Medium Range Incorporating Weather Model, Topography, Socio-Economic Information and
634 Land Use Exposure." *Advances in Water Resources* 146(April): 103785.
635 <https://doi.org/10.1016/j.advwatres.2020.103785>.

636 Tripathy, Shrabani S, Hari Vittal, Subhankar Karmakar, and Subimal Ghosh. 2020b. "Advances in Water
637 Resources Flood Risk Forecasting at Weather to Medium Range Incorporating Weather Model ,
638 Topography , Socio-Economic Information and Land Use Exposure." *Advances in Water Resources*
639 146(October): 103785. <https://doi.org/10.1016/j.advwatres.2020.103785>.

640 USACE. 2016. "HEC-RAS River Analysis System Hydraulic Reference Manual Version 5.0." *Hydrologic*
641 *Engineering Center* (February): 547.

642 Utazi, C. Edson et al. 2018. "High Resolution Age-Structured Mapping of Childhood Vaccination Coverage in
643 Low and Middle Income Countries." *Vaccine* 36(12): 1583-91.
644 <https://doi.org/10.1016/j.vaccine.2018.02.020>.

645 Wang, Yi et al. 2019. "A Hybrid GIS Multi-Criteria Decision-Making Method for Flood Susceptibility Mapping
646 at Shangyou, China." *Remote Sensing* 11(1).

Figures

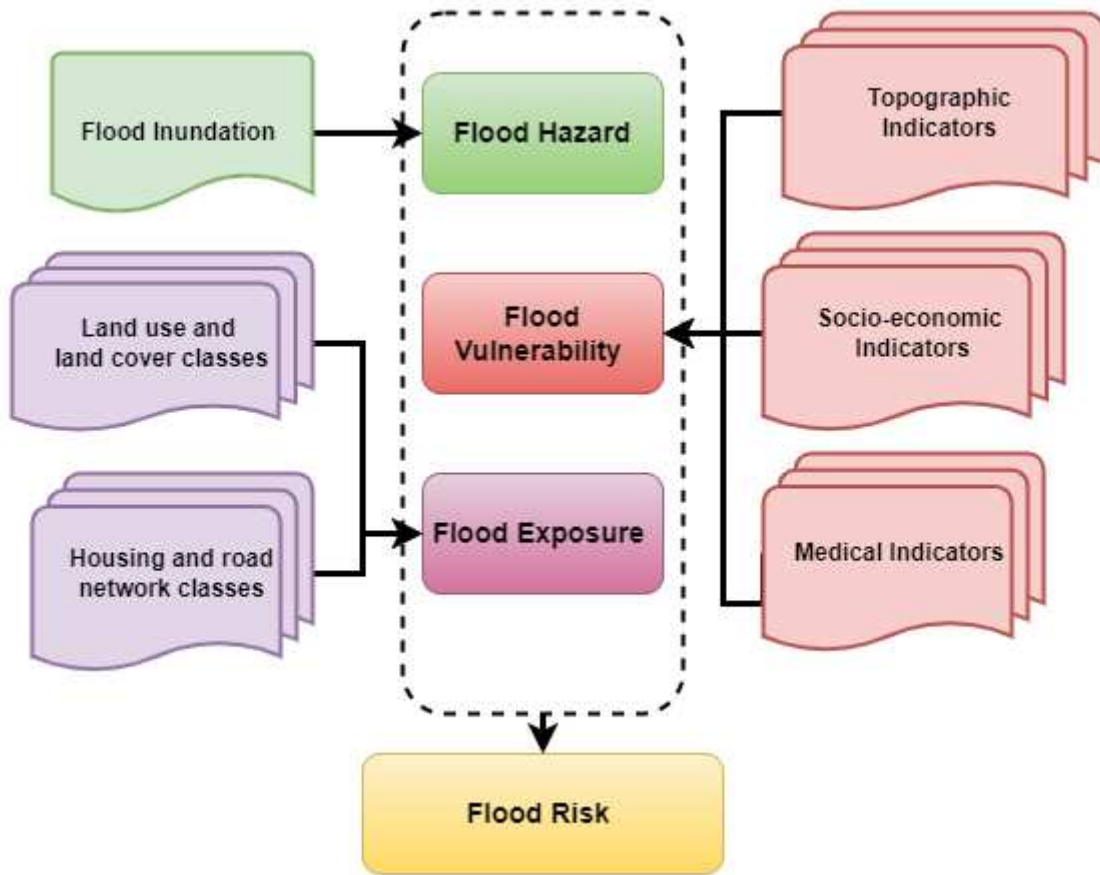


Figure 1

Flow chart depicting different steps involved for flood risk assessment.

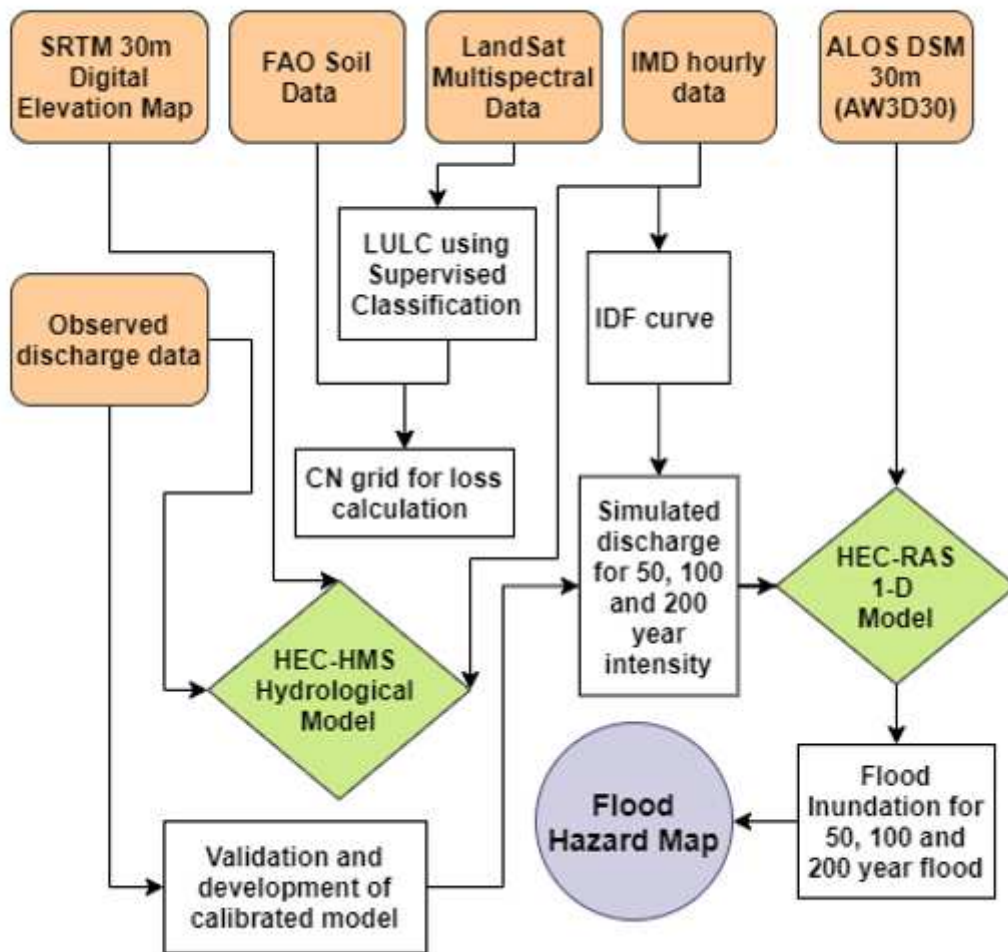


Figure 2

Flow chart depicting different steps involved for flood hazard mapping. The flow chart includes the input data for calculating the discharge for different return periods using HEC-HMS model and then the extent of flood inundation using the HEC-RAS model.

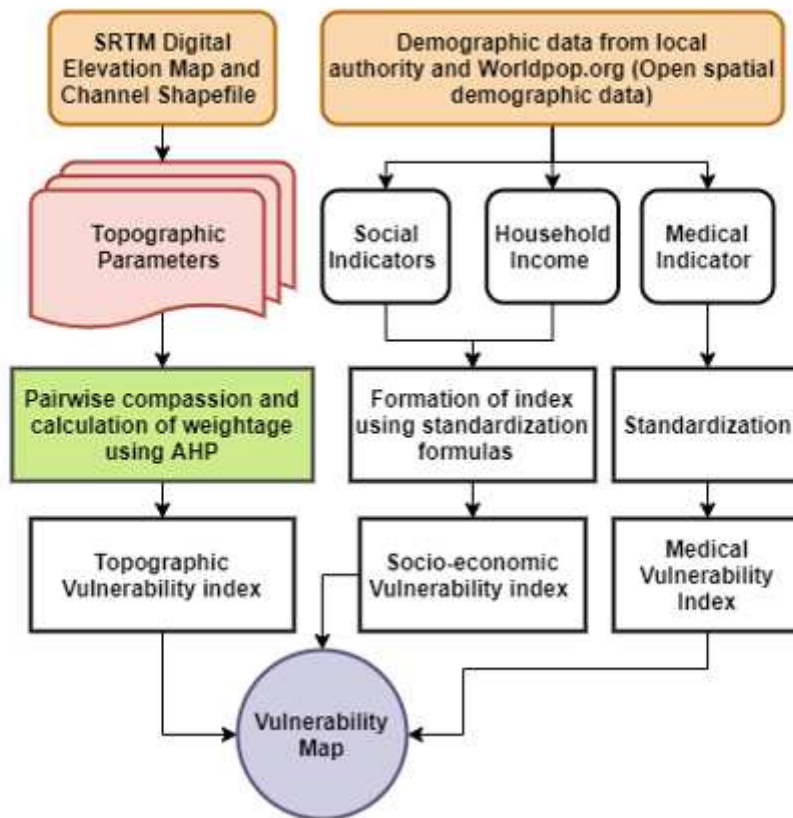


Figure 3

Flow chart depicting different steps involved for flood Vulnerability mapping. The vulnerability is calculated by considering topographic vulnerability and socio-economic vulnerability.

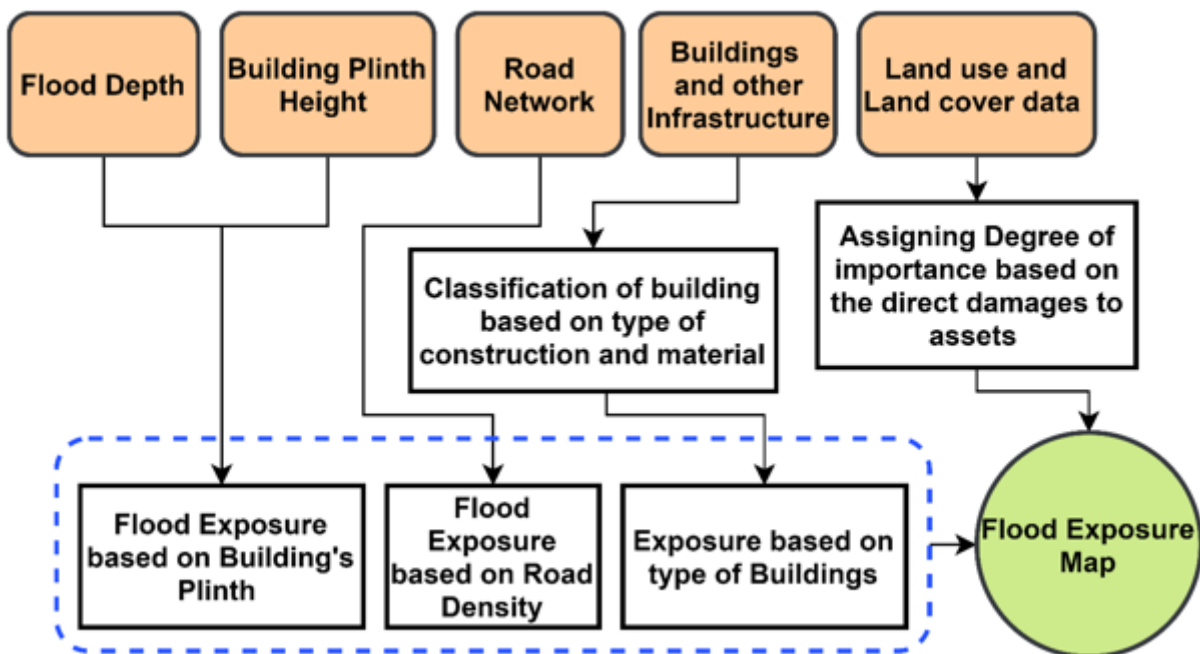


Figure 4

The flowchart depicting the steps for calculating the flood exposure. The exposure is calculated by considering building and infrastructure exposure, and land use and land cover exposure.

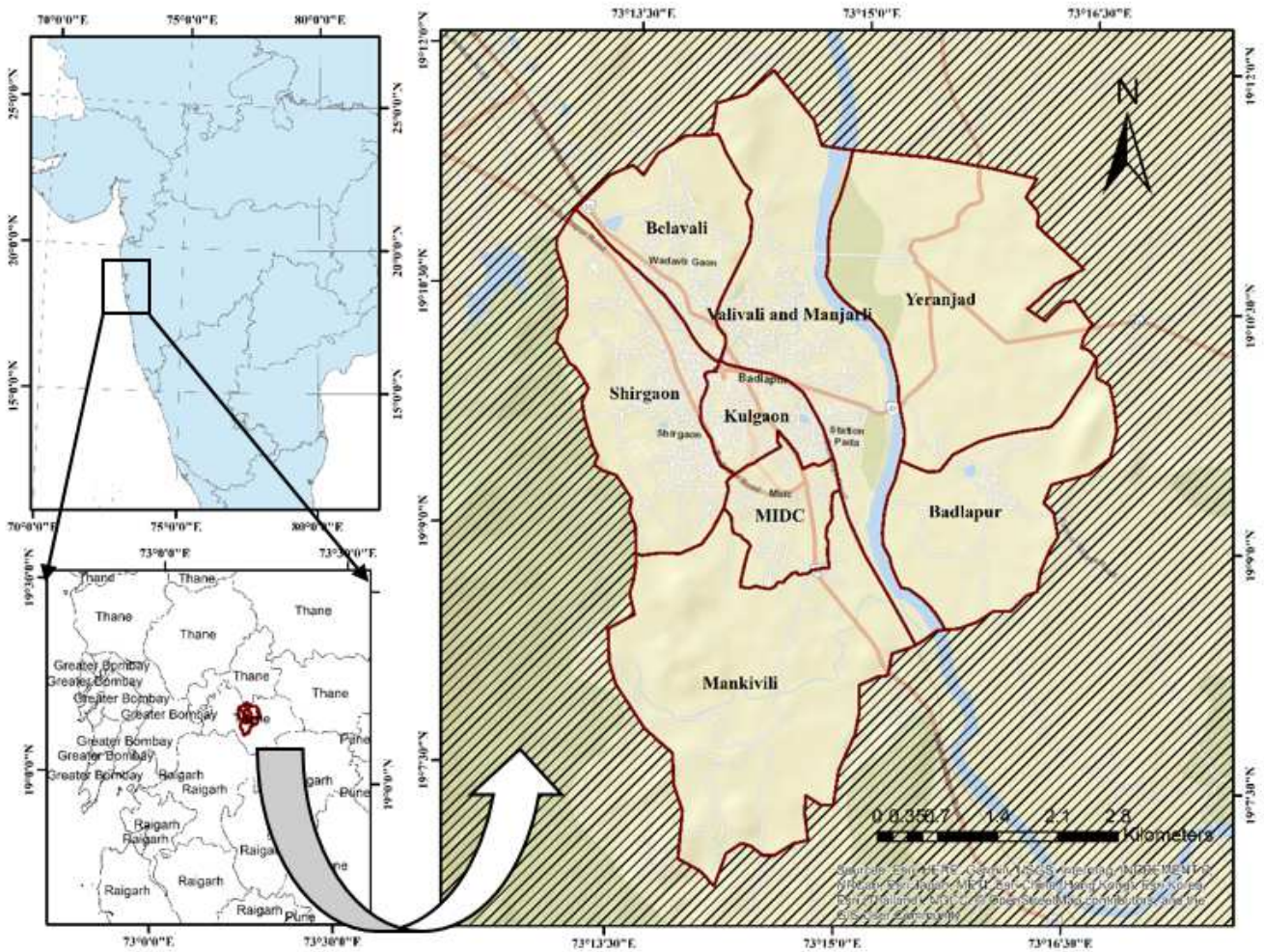


Figure 5

Location map of Kulgoan-Badlapur Municipal Council's (KBMC) area.

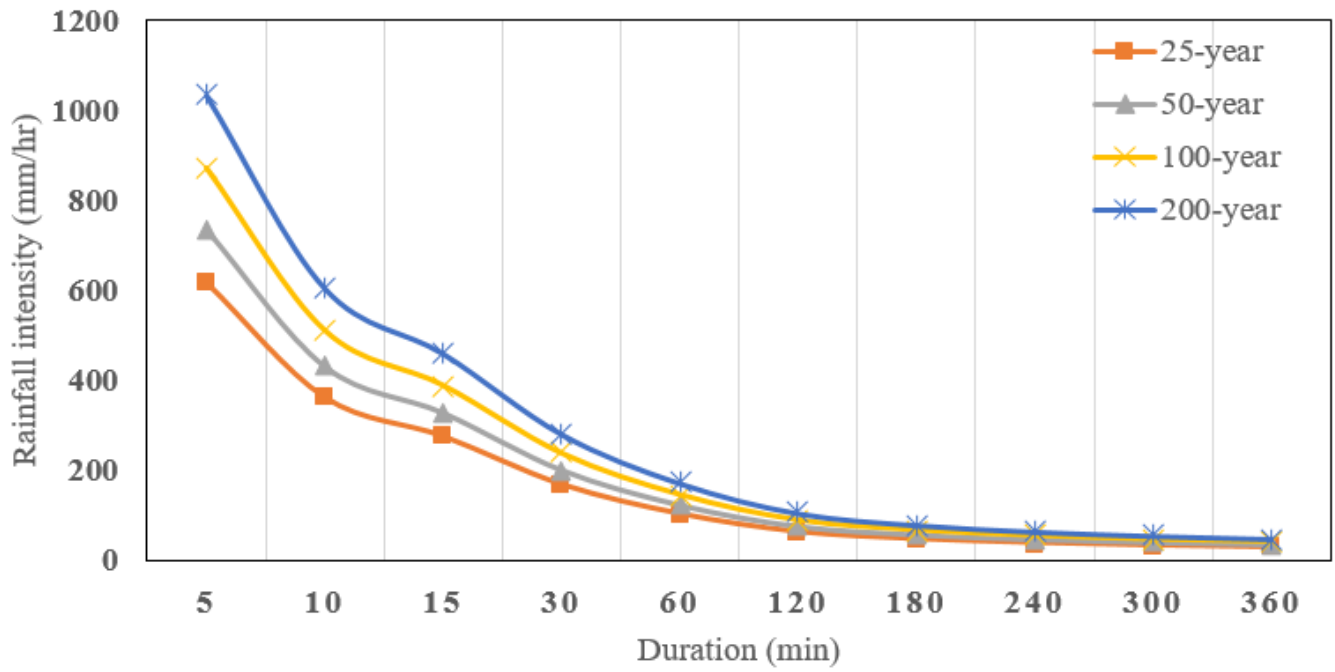


Figure 6

Intensity-Duration-Frequency (IDF) curves derived for Kulgaon-Badlapur Municipal Council (KBMC) area. The graph shows the intensity of the rainfall in mm/hr for 25-year, 50-year, 100-year, and 200-year return periods.

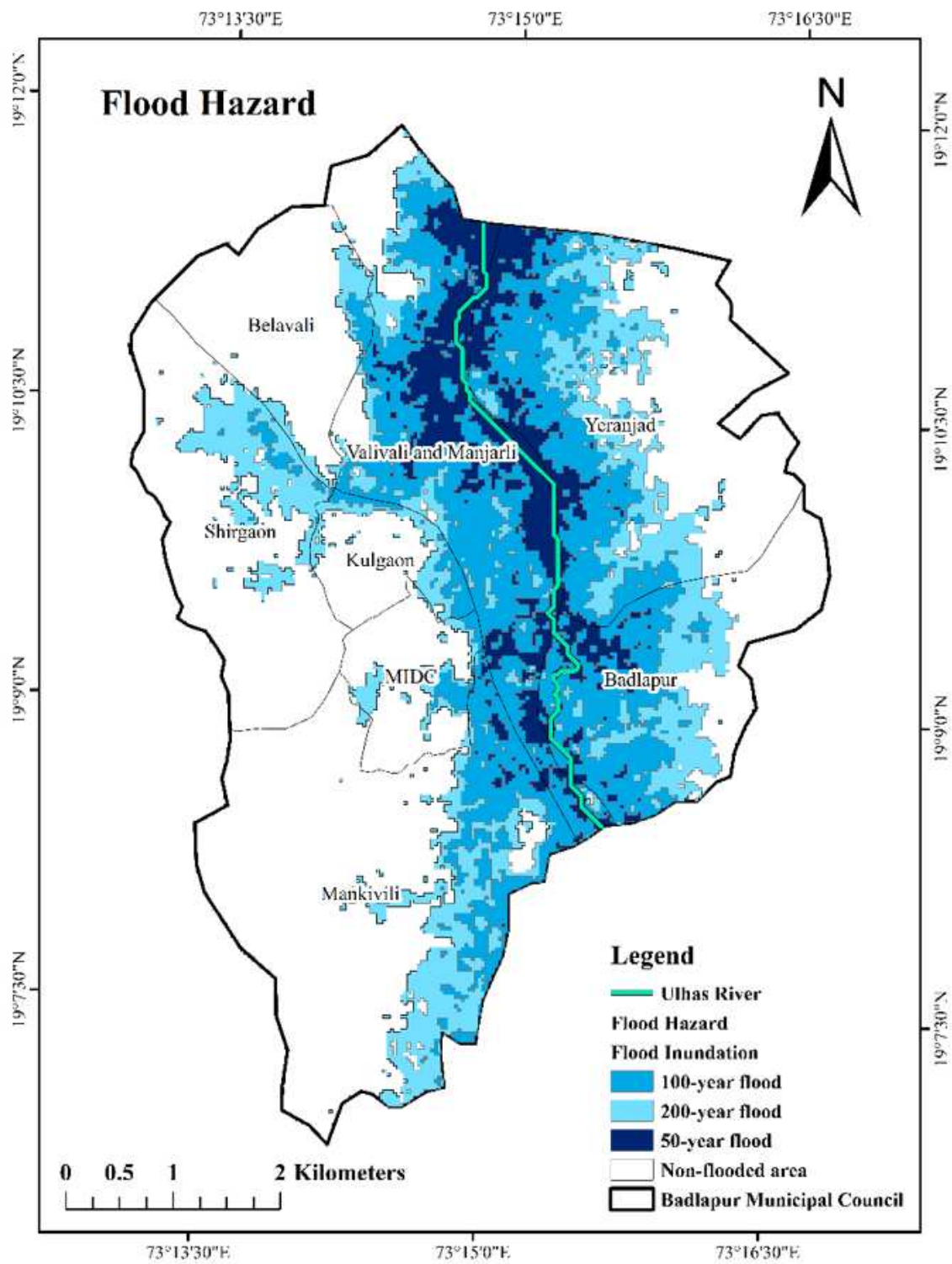


Figure 7

Flood hazard map for Kulgaon-Badlapur Municipal Council (KBMC). The flood hazard is calculated by determining the flood inundation associated with 50-year, 100-year and 200-year return periods.

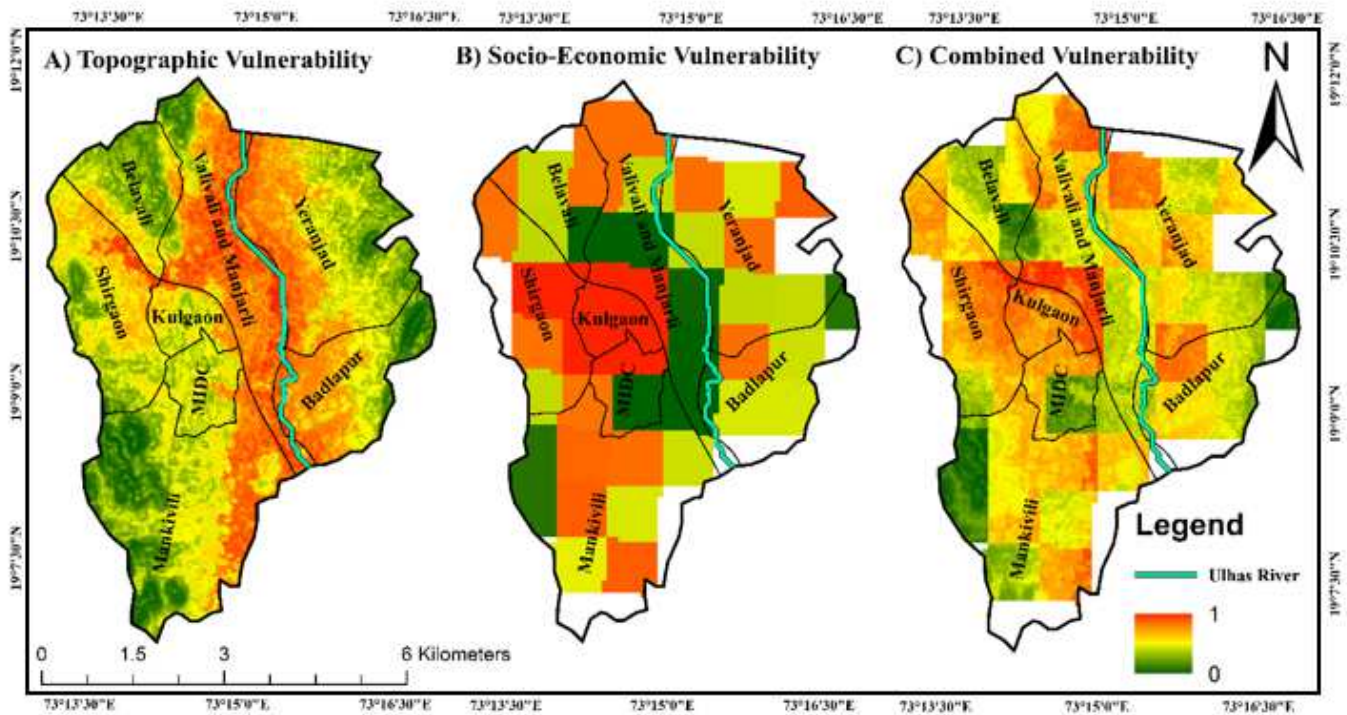


Figure 8

The maps showing spatial distribution of vulnerability in Kulgaon Badlapur Municipal Council (KBMC) area: (A) Topographic vulnerability map; (B) The socio-economic vulnerability map, obtained by combining the social, economic, and medical indicators; (C) The combined flood vulnerability map, obtained by combining the topographic and socio-economic vulnerability.

Figure 9

The flood exposure maps for the Kulgaon-Badlapur Municipal Council (KBMC) area, obtained by considering (A) the direct damages based on the land use and land cover classes; (B) based on the road network; (C) The flood exposure map, based on the combination of infrastructural exposure which is calculated by considering road density, plinth height, and type of building along with a degree of importance assigned to each land use and land cover class based on the probable direct damages.

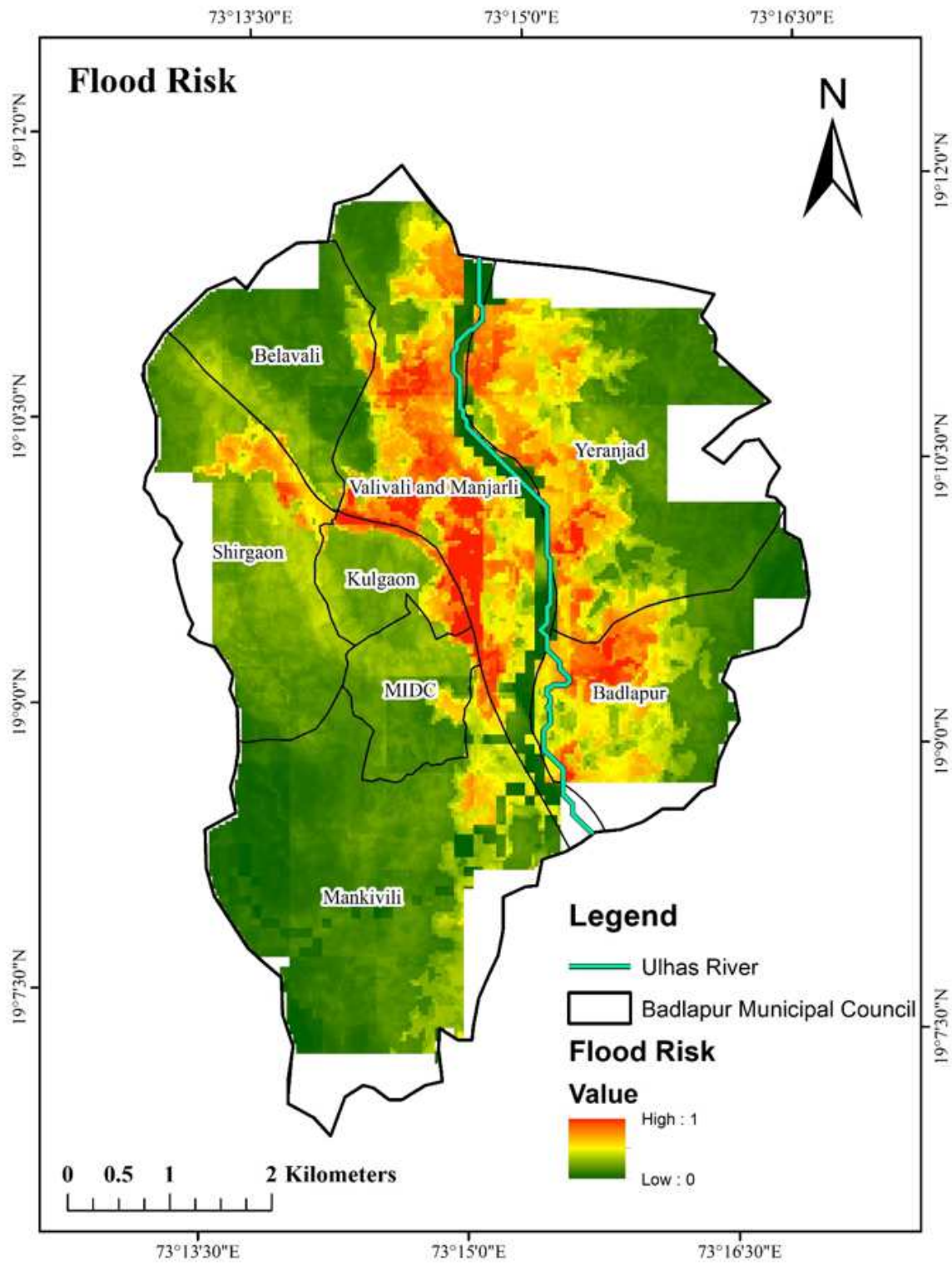


Figure 10

The flood risk map of Kulgaon-Badlapur Municipal council (KBMC) area. The risk is calculated by multiplying the flood hazard, vulnerability, and exposure.